Japan Bilingual Publishing Co.

New Environmentally-Friendly Materials

https://ojs.bilpub.com/index.php/nefm

ARTICLE

Efficient Photocatalytic Degradation of Crystal Violet Dye Using a Synthesized CdO:V2O5 Nanocomposite in the Presence of Sunlight

Sajid M. Mansoori

Department of Chemistry, Shri Vile Parle Kelavni Mandal's, Mithibai College of Arts, Chauhan Institute of Science & Amrutben Jivanlal College of Commerce and Economics (Autonomous) Ville-Parle (West), Mumbai 400056, India

ABSTRACT

Materials containing two or more separate phases, at least one of which has nanoscale dimensions, are called nanocomposites. Coupled semiconductor metal oxides have drawn a lot of interest among these because of their special and improved physicochemical characteristics. These characteristics frequently result from changes in the density of states, electron tunneling, surface plasmon resonance, and quantum confinement effects. In this work, a straightforward and economical co-precipitation technique was used to create CdO:V_2O_5 binary metal oxide nanocomposites. The presence of crystalline phases corresponding to both CdO and V_2O_5 was confirmed by X-ray diffraction (XRD), which was used to evaluate the structural properties of the resultant nanocomposites. The Debye-Scherrer formula was used to compute the crystallite sizes, which showed that the particles were in the nanoscale range and had high crystallinity. The degradation of crystal violet dye under visible light was used to assess the produced nanocomposites' photocatalytic activity. To investigate the impact of composition on photocatalytic efficiency, nanocomposites with CdO:V_2O_5 molar ratios of 1:1, 1:2, and 2:1 were investigated. First-order kinetics was confirmed by the regression coefficients for the degradation process, which were 0.9919, 0.9903, and 0.9800, respectively. The two semiconductors' synergistic interactions, which improve charge separation and light absorption, are responsible for the difference in photocatalytic performance. These findings imply that CdO:V_2O_5 nanocomposites are potential options for effective photocatalytic applications, particularly in environmental remediation and wastewater treatment, especially when used at optimal ratios.

Keywords: Metal Oxide Nanocomposites; Co-precipitation; Crystal Violet; Photo-degradation

*CORRESPONDING AUTHOR:

Sajid M. Mansoori, Department of Chemistry, Shri Vile Parle Kelavni Mandal's, Mithibai College of Arts, Chauhan Institute of Science & Amrutben Jivanlal College of Commerce and Economics (Autonomous) Ville-Parle (West), Mumbai 400056, India; Email: mohd.mansoori@mithibai.ac.in

ARTICLE INFO

Received: 21 March 2025 | Revised: 26 April 2025| Accepted: 3 May 2025 | Published Online: 10 May 2025

DOI: https://doi.org/10.55121/nefm.v4i1.413

CITATION

Mansoori, S.M., 2025. Efficient Photocatalytic Degradation of Crystal Violet Dye Using a Synthesized CdO:V2O5 Nanocomposite in the Presence of Sunlight. New Environmentally-Friendly Materials. 4(1): 23–34. DOI: https://doi.org/10.55121/nefm.v4i1.413

1. Introduction

Research on nanoparticles, especially in powder form, is currently gaining attention because of their superior thermal, magnetic, optical, and electrical properties when compared to their bulk counterparts [1]. These nanopowders also exhibit strong antibacterial and photocatalytic activity because of their size, shape, and surface characteristics [2]. Recently, metal oxide nanopowders have been found to play a significant role in materials research, chemistry, and physics [2–3]. The n-type II-VI semiconductor cadmium oxide nanomaterial has an indirect bandgap of 1.98 eV and a direct bandgap of 2.5 eV [2]. The processes and conditions used to produce CdO nanoparticles affect their stoichiometry, particle size, and shape [3]. Numerous techniques have been used to produce cadmium oxide nanoparticles [4–11].

The physical and chemical characteristics of cadmium oxide nanoparticles were enhanced by altering the manufacturing processes [12]. The co-precipitation process has been demonstrated to be successful in producing a variety of nanostructures among the other techniques [13]. Cadmium oxide nanoparticles are characterized by large band gaps, low electrical resistance, and strong transmission in the visual spectrum. The properties of cadmium oxide nanoparticles are distinct [14]. Consequently, common applications include phototransistors, photodiodes, catalysts, solar cell manufacturing, optoelectronic devices, and nonlinear materials [15–16].

CdO was selected as the preferred material due to its excellent stability, broad availability, and affordable price. In addition, CdO has interstitial cadmium atoms and oxygen vacancies, which contribute to its good optical qualities and low electrical resistance [7]. which all have relevance to photocatalysis. It is also appropriate for visible-light dye degradation due to its precisely matched visible band-gap. By changing the manufacturing process, several researchers are trying to improve the chemical and physical properties of CdO.

Vanadium pentoxide V_2O_5 is used in solar cell windows, solid-state batteries, chemical sensors, catalysis, and electrochromic devices . The band gap (Eg) of the diamagnetic semiconductor V_2O_5 is around 2.3 eV [8-11]. Much effort has been made to create meso- and nanostructured V_2O_5 in order to enhance its advantageous properties. For instance, nanorods and nanowires are fascinating because of their small radial dimensions, which enable them to exhibit distinctive characteristics while maintaining a wire-like connection. For instance, V_2O_5 nanotubes are ideal as electrodes in Li batteries due to their increased redox reaction capacity and larger specific surface area. Field emission properties of arrays of hydrated vanadium pentoxide nanotubes are good [3]. Additionally, nanostructured materials have been used to produce nano actuators and nonlinear optical limiters [4].

Because of its important optical, physical, and chemical properties, the fabrication of group II-VI semiconductor binary chalcogenides in nanopowder form has been a rapidly growing subject of study. Interest is growing in the real-world uses of II-VI semiconductor nanoparticles, such as optoelectronics and zero-dimensional quantum bound materials. Semiconductor nanoparticles are a specific type of material used in the manufacturing of semiconductors [5].

The size of these nanoparticles affects their chemical and physical characteristics. Large-scale production, such as solid powder, is required for the investigation of the physical characteristics of semiconductor nanoparticles and for industrial uses in microelectronics, photocatalysis, and catalysis. Combining different semiconductor oxides or creating nanohybrids may result in a smaller band gap, which extends the absorbance range to the visible light spectrum. Additionally, when electron-hole pairs separate during irradiation, this leads to increased photocatalytic activity [18-23]. There are two different energy-level systems in hybrid semiconductor materials, and both are crucial for charge separation.

Organic contaminants are degraded more quickly in these systems as well. Different linked semiconductors have been successfully produced. They include ZnO/TiO_2, TiO_2/WO_3, TiO_2/SnO_2, TiO_2/MgO, CdS/ZnO. CdS/ZnO and ZnO–Al_2O_3 reduced graphine oxide [24,26–29]. Methylene blue (MB) photocatalytic degradation was improved in V_2O_5/ZnO heteronanorods [30]. ZnO-CuO nanocomposites showed a 20–30% increase in MB degradation when compared to pure ZnO and CuO.

Photocatalysis has garnered a lot of attention worldwide as a result of the recent prominence of water pollution from numerous enterprises. Almost all textile manu-

facturers have discharged synthetic and artificial color dye pollution into the environment as effluent. Because textile effluents contain a variety of organic dye compounds that are poisonous, carcinogenic, and non-biodegradable, they are a significant source of water pollution. Both the environment and live organisms are at risk from these substances. Therefore, creating cost-effective and efficient wastewater treatment methods is more important than ever. Membrane filtration, adsorption, flocculation, coagulation, and—above all—photocatalytic destruction has all been used to clean water in the past [1–2,31].

The structural, morphological, spectroscopic, and photocatalytic investigations of the CdO/V_2O_5 nanocomposite were investigated in this work, and the results are detailed.

2. Materials and Methods

S.D. Fine Chem. Limited provided analytical-grade sodium hydroxide, ethanol, methanol, ammonium metavanadate, and cadmium nitrate hexahydrate, which were utilized without additional purification.

2.1. Synthesis of CdO/V_2O_5 Nanocomposites

A simple co-precipitation procedure utilizing ammonium metavanadate and $Cd(NO_3)_2 \cdot 6H_2O$ yielded a $CdO:V_2O_5$ nanocomposite. The nanocomposites are prepared as per the distribution given in the following **Table 1**.

Table 1. Distribution of mole ratio for $CdO:V_2O_5$.

Sr. No.	Mole ratio	Cadmium nitrate (millimole)	Ammonium metavanadate (millimole)	Indexing
1	1:1	1	1	Cdv
2	1:2	1	2	cdv2
3	2:1	2	1	cd2v

The metal ion solution was treated with 4N (4 normal) sodium hydroxide to produce a precipitate. The precipitate was filtered and washed thoroughly with distilled water many times. Methanol was used for the final wash. The precipitate was dried for 24 hours in an electrical oven at 110°C. The dried samples were calcined for 6 hours at 500°C in a tube furnace [11–14]. The synthesize material is solid in nature. The molar ratio of the CdO/V_2O_5 nanocomposites was labelled cdv($CdO:V_2O_5$), cdv2($2CdO:2V_2O_5$), and cd2v($CdO:V_2O_5$) on the synthesized products. Flow chart is represented in **Figure 1**.

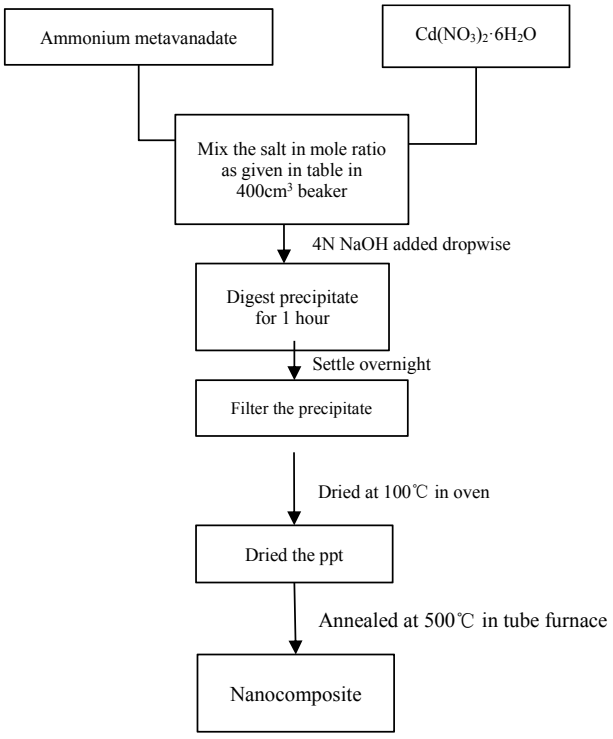

Figure 1. A flowchart depicting the $CdO:V_2O_5$ Nanocomposites synthesis process.

2.2. Structural Characterization

A UV-Vis spectrophotometer (systronic UV-2203) was used to measure the optical absorption spectra in the 300–800 nm region. A Shimadzu XRD-7000 was used to gather X-ray diffraction patterns in the 2theta 10 nm to 80 nm region using CuKα, the radiation wavelength (λ = 0.15406 nm).

2.3. Calibration Curve

To discover linear regression coefficients, the linearity of the analysis response is examined. The limit of detection (LOD) and limit of quantitation (LOQ) are calculated using the blank determination technique. When a large number of standards are run, a calibration curve is often created by plotting the signal from the standard analysis against the standard concentration. Over a range of concentrations, the relationship between the signal and concentration is often linear (i.e., the signal is exactly proportional to concentration), and a linear least-squares line

is used to fit the data. In the most common type of least-squares analysis, the distance between data points and the line down the y-axis is minimized. This presumes that the values for the x-coordinates have far less inaccuracy than the values for the y-coordinates value [23–24].

A calibration curve was developed from a set of reference samples with known crystal violet concentrations. The calibration line, which was constructed from 15 standard solutions to find the linear regression coefficient, LOQ and LOD.

The linearity of the analysis response was checked using the linearity of the calibration line, which was produced from 15 standard solutions (0.01 ppm to 10 ppm). Dissolve 100 milligrams of crystal violet dye in 1000 cm^3 of distilled water to prepare a 100ppm crystal violet dye (stock solution).

Preparation of a series of solutions: As shown in the **Table 2**, a series of typical crystal violet solutions have been prepared.

For measuring the quantity of crystal violet in unknown samples following photocatalytic degradation of the solution, a calibration curve was developed from a set of reference samples with known concentrations of crystal violet. Absorbance is recorded at 595 nm (λ_{max}) using a spectrophotometer (Systronic 2203). Using the blank determination technique, the limit of detection (LOD) and limit of quantitation (LOQ) were determined.

The reproducibility of six duplicate measurements of 0.1 ppm crystal violet in terms of relative standard deviation (RSD) in percentage was determined.

Table 2. Preparation of Crystal Violet solutions.

Concentration of CV (ppm)	Volume of stock solution (100 ppm) in cm^3	Amount of water in cm^3	Final volume of solution in cm^3
0.01	0.01	99.99	100
0.02	0.02	99.98	100
0.04	0.04	99.96	100
0.06	0.06	99.94	100
0.08	0.08	99.92	100
0.1	0.1	99.9	100
0.3	0.3	99.7	100
0.5	0.5	99.5	100
0.7	0.7	99.3	100
1	1	99	100
3	3	97	100
5	5	95	100
7	7	939	100
9	9	91	100
10	10	90	100

2.4. Photocatalytic Activity Studies

Under the influence of sunlight, the photocatalytic degradation of crystal violet was carried out in a 250 cm^3 conical flask using synthesised CdO/V_2O_5 as a photocatalyst at various time intervals. Before exposure to sunlight, 10 mg of synthesised CdO/V_2O_5 powder was equilibrated with 50 cm^3 of 10ppm crystal violet dye solution by shaking on a shaker for 30 minutes, i.e., $CdO:V_2O_5$. A UV–visible spectrophotometer (systronic UV-2203) was used to study the photocatalytic breakdown of crystal violet in a 5 mL sample at regular time intervals.

The decolorization and degradation efficiency (D) were calculated using the equation below:

$$D = 100 \times (C_0 - C_t/C_0) \quad (1)$$

where C_0 denotes the dye solution's initial concentration in ppm and Ct signifies the dye solution's final concentration

in ppm after irradiation at the given time interval (t) [29,30].

Following the degradation process, the catalyst was collected using filter paper to measure the activity of the recycled catalysts. The fresh crystal violet solution and recovered catalyst were used in the following run [31,32]. The experiment was repeated five times.

3. Results and Discussion

Figure 2 shows the FTIR spectrum of the CdO/V_2O_5 nanocomposite. The absorption bands at 505 and 620 cm^{-1} are caused by V_2O_5 and Cd-O stretching vibrations, respectively. The O-H group's water vibrations are attributed to the bands at 1644 and 3432 cm^{-1}.

The unique bands in the 400–700 cm^{-1} range correlate to the Cd-O mode. Peaks at 534 cm^{-1} and 545 cm^{-1} indicate Cd-O bonding. The peak due to Cd-O stretching vibration may be seen at 688 cm^{-1}. The large absorption band at 858 cm^{-1} [28] demonstrates the existence of the Cd-O bond. Oxygen stretching is responsible for the frequency at 1,000 cm^{-1}.

There are no other bands visible in the spectra, indicating that only metal-oxygen functional groups are present. Asymmetric stretching V-O-V corresponds to 727 cm^{-1}. Vanadium oxide for V_2O_5 powder represents the stretching vibrations of terminal oxygen bonds (V = O), doubly coordinated oxygen (bridge oxygen) bonds, and the asymmetric and symmetric stretching vibrations of triply coordinated oxygen (chain oxygen) bonds at 1018 cm^{-1}, 829 cm^{-1}, 611 cm^{-1}, and 476 cm^{-1}, respectively.

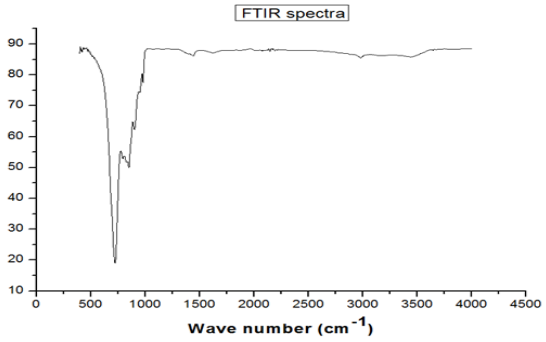

Figure 2. FTIR spectra of prepared nanocomposite.

XRD pattern of prepared nano composite is seen in **Figure 3**. The XRD pattern of CdO nanopowders is shown in this picture. The cubic crystal structure of pure CdO, as shown on JCPDS Card No. 65-2908, closely fits all of the diffraction peaks in terms of location and order of intensities. The strong and powerful peaks indicate that the nanopowder is crystalline. The (111), (2 0 0), (2 2 0), (3 1 1), and (2 2 2) planes were assigned to peaks at 2theta values of 32.994, 38.279, 55.265, 65.820, and 69.239, respectively.

The diffracted peaks at 32.27°, 33.56°, 38.83°, 50.27°, 55.74°, 58.42°, 66.38°, and 69.76° (JCPDS file No. #651085) are indexed to the cubic crystalline structure of CdO with lattice parameter a = b = c = 6.48.

The XRD patterns indicated sharp peaks 2 angle at the peak position of 25.2°, 32°, 33.5°, 37.5°, 45°, and 51° with (101), (400), (011), (301), (411) and (002) diffraction planes, respectively, which are consistent with the rhombohedral structure of the V_2O_5 phase.

According to the XRD analysis, the prepared nanocomposites contained a significant amount of crystalline CdO/V_2O_5 . The average crystallite size is computed using the Debye–Scherer formula from the full width at half maximum (FWHM) of the diffraction peaks and is found to be between 20 and 40 nm [18].

$$\text{Average particle size (D)} = 0.9\lambda/\beta\cos\theta \qquad (2)$$

where, X-ray wavelength is represented by λ, and D is the size of the crystalline particle. The broadening of the diffraction peak (β) and θ is angle of diffraction.

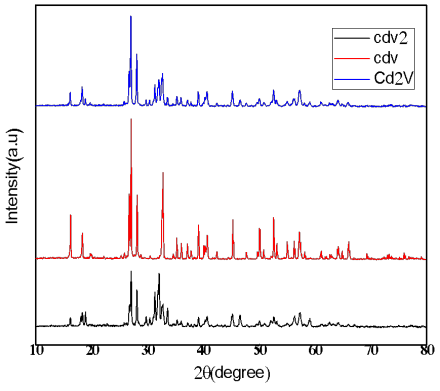

Figure 3. XRD spectra of CdO/V_2O_5 nanocomposite of CdV_2, Cd_2V and CdV.

Average particle size of nanocomposites is between 24 nm to 38 nm as mention in **Table 3**. An increase in the molar ratio of cadmium in composite doesn't affect the particle size; however, increasing the mole ratio of vanadium decreases the size of the particle from 40 nm to 25 nm.

Table 3. Particle size of nanocomposite.

Sample	Average particle size
CdV	37.1446
CdV_2	24.88
CdV_2	29.619

Field emission scanning electron Microscopy (FESEM) imaging was used to examine for the one sample [((1:1) CdO/V_2O_5] to understand the morphology of synthesised nanocomposite. The image revealing an agglomerated structure-like morphology as seen in **Figure 4**.

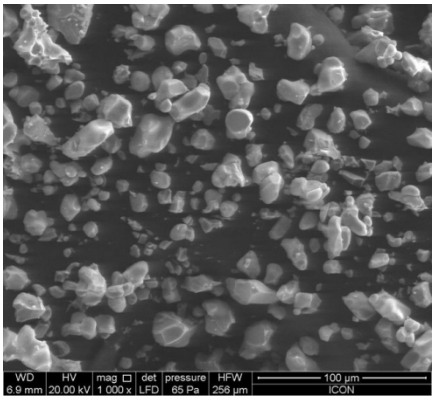

Figure 4. SEM of CdO:V_2O_5 nanocomposites (1:1).

For measuring the quantity of crystal violet in unknown samples following photocatalytic degradation of solution, a calibration curve (**Figure 5**) was developed from a set of reference samples with known crystal violet concentrations. The calibration line, which was constructed from 15 standard solutions with a linear regression coefficient of 0.9957 and a slope of 0.0847, was used to test the linearity of the analytical response. (See **Figure 3**) Using the Blank determination technique, the limit of detection (LOD) and limit of quantitation (LOQ) were calculated and found to be 0.052393 mg/L and 0.19635 mg/L, respectively.

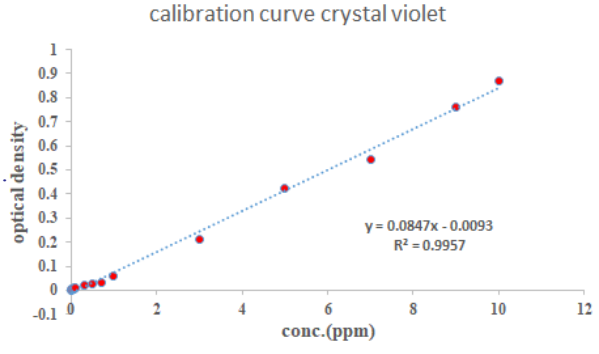

Figure 5. The calibration curve for crystal violet.

The least-squares line has a slope of b = 0.08468 and an intercept of a = –0.0093.

y = 0.08468x – 0.0093 is the regression line's equation.

Random errors in the Y-direction, Sy/x = 0.020565.

Limit of Detection (LOD),

$$LOD = yB + 3SB \quad (3)$$

Limit of Quantification (LOQ),

$$LOQ = yB + 10SB \quad (4)$$

where yB (= a) is a blank signal and SB(Sy/x) is the standard deviation of the blank.

Hence,

LOD= –0.0093 + 3 × 0.020565 = 0.052393 mg/L

LOQ = –0.0093 + 10 × 0.020565 = 0.19635 mg/L

Relative standard deviation (RSD) in percentage was calculated using six replicate measurements of 0.1 ppm crystal violet and was found to be 0.0%. Represented in **Table 4** [31].

Table 4. Results of repeatability studies at concentration 0.1 ppm.

Sr No.	Absorbance	$\bar{x}$	SD	RSD
1	0.012	0.012	0.00	0.00%
2	0.012			
3	0.012			
4	0.012			
5	0.012			
6	0.012			

Results of repeatability studies confirm that the response of the instrument has good agreement with respect to concentration of crystal violet dye solution, and shows no error in the measurement [32,33].

The degradation of crystal violet was studied using CdO/V_2O_5 nanocomposites with molar ratios of 1:1, 1:2, and 2:1. At 180 minutes, the maximum degradation efficiency for a CdO/V_2O_5 was 80.99 percent. As shown in **Figure 6**, the degradation of crystal violet was 76.125 percent for a 1:1 ratio, 68.95 percent for a 1:2 ratio of CdO/V_2O_5, and 79.162 percent for a 3:1 ratio of CdO/V_2O_5. As a result, the current investigation on crystal violet degradation utilising V_2O_5 nanocomposites reveals that increasing the ratio of CdO to V_2O_5 favours charge separation, and

hence degradation is better than when mole ratio of V_2O_5 is more than CdO.

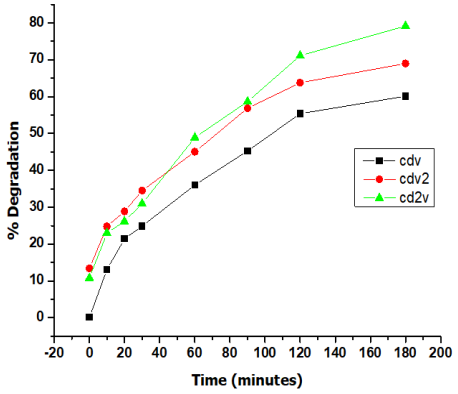

Figure 6. Plots of crystal violet dye percentage degradation as a function of time when exposed to visible light.

The plot's linearity indicates that the degradation process of crystal violet dye utilising the nanocomposite CdO:V_2O_5 as a catalyst at 1:1, 1:2, and 2:1 exhibits good agreement with first-order kinetics, with regression values of 0.9957, 0.9903, and 0.9800, respectively [31,32].

The linearity of the plot shows that the Degradation reaction of CV dye using CdO:V_2O_5 (1:1) (**Figure 7**), CdO:V_2O_5 (2:1) (**Figure 8**) and CdO:V_2O_5 (1:2) (**Figure 9**) nanocomposite as catalyst follows first order kinetics.

Under visible light irradiation, the photocatalytic activity of nanocomposites with CdO:V_2O_5 molar ratios of 1:1, 1:2, and 2:1 exhibits strong photoresponse and follows first-order kinetics with regressions of 0.9957, 0.9903, and 0.9800, respectively. The improved photocatalytic activity of the prepared nanocomposite might be due to the increased percentage of CdO with respect to V_2O_5 in the nanocomposite [8–12]. Comparative data is given in the **Table 5**.

The photons eject electrons from the valence band (VB) of the catalyst surface and move to the conduction band (CB). The recombination occurs between the electron and the hole itself or by the surface charges. Precisely controlling the recombination rate measures the performance of photocatalysis. Band gap, average crystallite size, specific surface area, and defect or localised states are a few of the aspects that need to be taken into account in order to comprehend the mechanism of photocatalysis. These aspects are connected to the catalyst's composition and the characteristics of the target pollutants. Based on related literature reports, degradation of CV by CdO:V_2O_5 nanocomposites under visible light [34–38]. The possible mechanism of degradation of pollutants using the catalyst and dye CV is illustrated in **Figure 10**.

Under visible light, V_2O_5 creates electron-hole pairs photo-generated electrons (e^-) can be transferred from the CB of V_2O_5 to the CB of CdO. The photocatalytic efficiency is enhanced by $O_2^{\bullet-}$, which could be generated due to the interaction of O_2 molecules with electrons. In addition, V_2O_5 reacts with photo-generated electrons and produces VO ions. Additionally, superoxide radicals are produced when dissolved oxygen interacts with surface-bound and/or Cd^{2+} ions. It is believed that the contribution of electrons to the synthesis of Cd^{2+} ions reduce the likelihood of electron-hole recombination and promotes the generation of hydroxyl radicals. Moreover, oxidation of water molecules by the holes generates $HO^{\bullet}$. Thus, $HO^{\bullet}$ and $O_2^{\bullet-}$ are generated due to electron and hole (e^-/h^+) transfers. These molecules have a powerful ability to break down CV molecules' bonds, which ultimately results in mineralization. The CdO:V_2O_5 surface can also be used to directly oxidise CV, removing it from the solution

According to the findings, the ratio of V_2O_5 to CdO in nanocomposites has a significant influence on crystal violet photocatalytic activity. The production of a (2:1) CdO:V_2O_5 nanocomposite allows for regulated recombination of photo-generated electrons and holes, which aids in improved degradation.

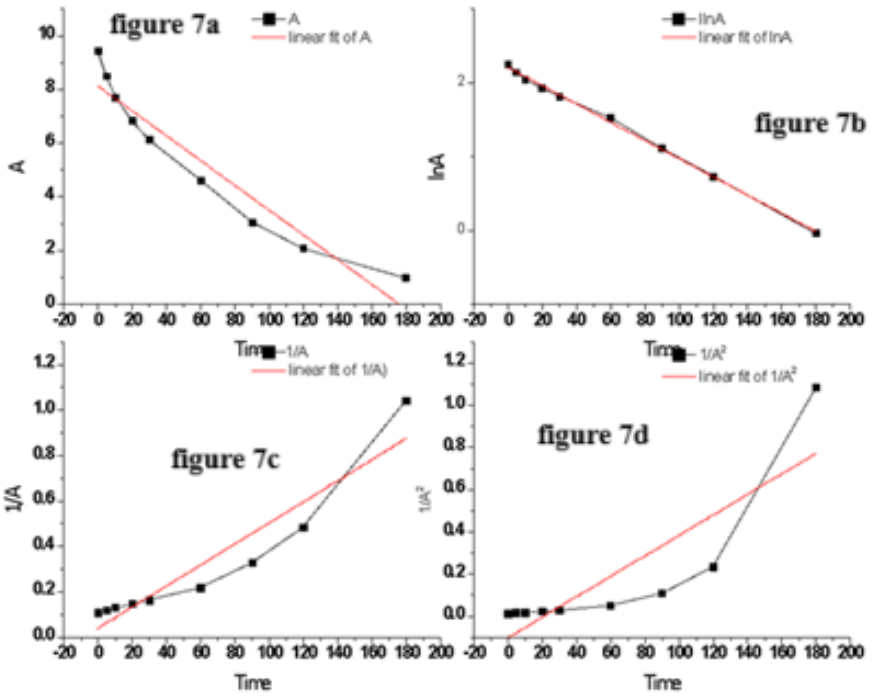

Figure 7. CdO/V_2O_5 (1:1) nanocomposite degradation of crystal violet (**a**) zero-order reaction (**b**) first-order reaction (**c**) second-order reaction (**d**) third-order reaction plot.

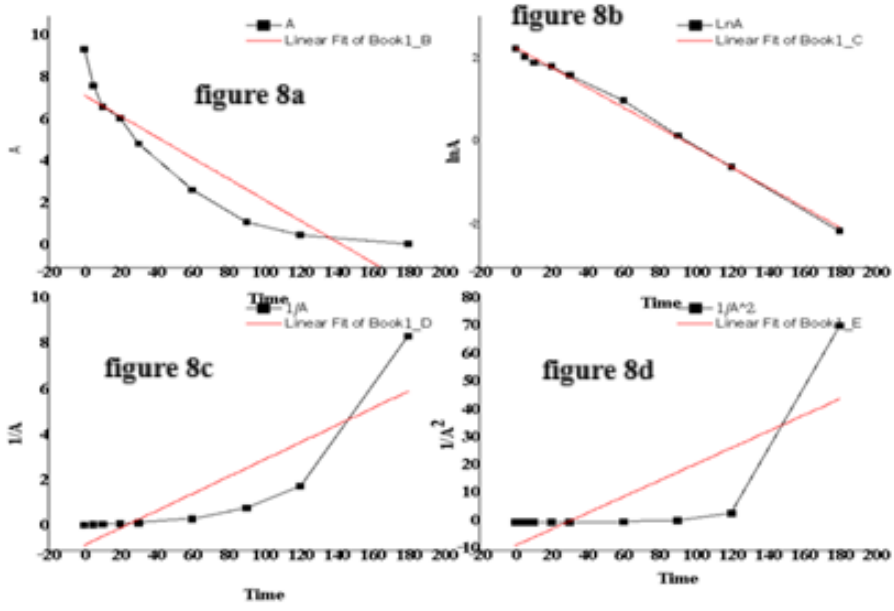

Figure 8. CdO/V_2O_5 (2:1) nanocomposite degradation of crystal violet (**a**) zero-order reaction (**b**) first-order reaction (**c**) second-order reaction (**d**) third-order reaction plot.

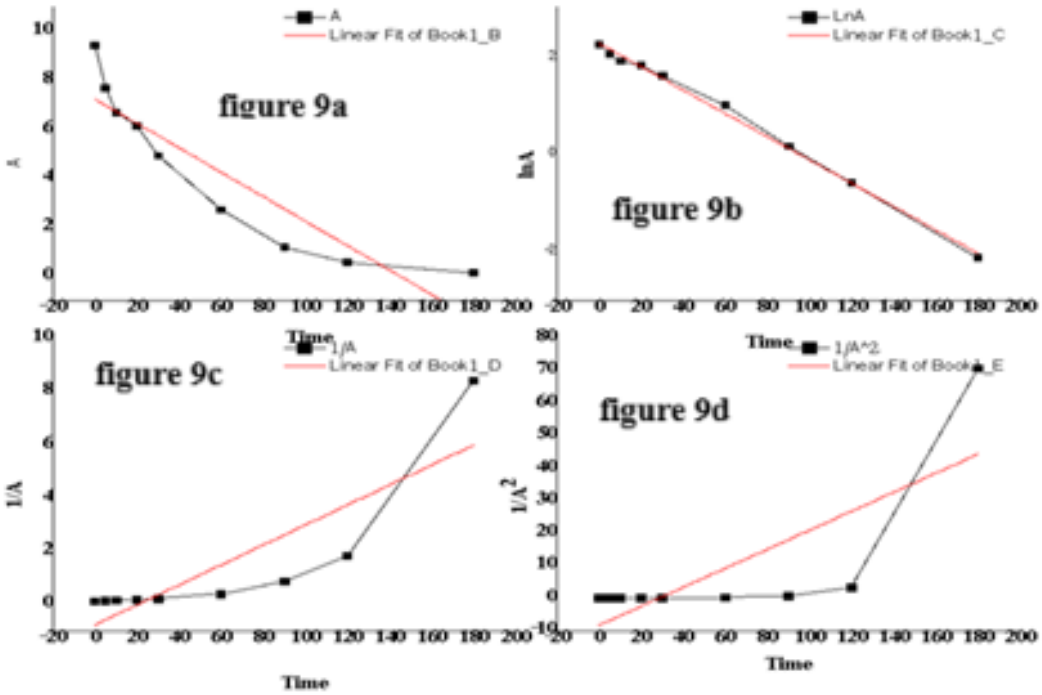

Figure 9. CdO/V_2O_5 (1:2) nanocomposite degradation of crystal violet (**a**) zero-order reaction (**b**) first-order reaction (**c**) second-order reaction (**d**) third-order reaction plot.

Table 5. Regression data of prepared binary metal oxide nanocomposite.

Metal oxide	Ratio	Zero order	First order	Second order	Third order
$CdO:V_2O_5$	1:1	0.9464	0.9957	0.9732	0.9013
$CdO:V_2O_5$	1:2	0.8548	0.9903	0.9857	0.9407
$CdO:V_2O_5$	2:1	0.8899	0.9800	0.9788	0.9044

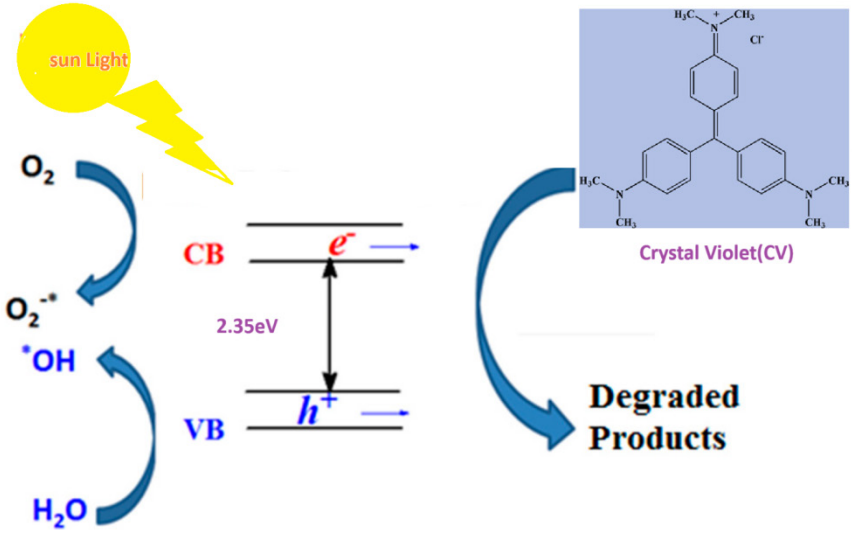

Figure 10. possible mechanism of degradation of pollutants using the $CdO:V_2O_5$ and dye CV.

4. Conclusions

$CdO:V_2O_5$ nanocomposites were effectively produced by a simple co-precipitation approach. The appearance of strong distinctive peaks in X-ray diffraction (XRD) study demonstrated that nanoscale $CdO:V_2O_5$ composites had formed. Under visible light, the nanocomposites' photocatalytic performance was assessed using varying molar ratios of CdO to V_2O_5 (1:1, 1:2, and 2:1). With regression values of 0.9957, 0.9903, and 0.9800, respectively, the data showed a robust photoresponse and first-order kinetics. The higher the CdO content in the composites, the higher the photocatalytic efficiency. In contrast to pure V_2O_5, which had a lower efficiency of 54.63%, the degradation efficiencies for $CdO:V_2O_5$ at molar ratios of 2:1, 1:1, and 1:2 were 78.78%, 75.75%, and 68.62%, respectively. The synergistic combination of CdO and V_2O_5, which enhances light absorption and charge separation, is responsible for this increased activity. $CdO:V_2O_5$ nanocomposites are interesting options for wastewater treatment and environmental remediation because of their efficiency and inexpensive production. Optimizing synthesis parameters and investigating wider uses for these materials should be the main goals of future studies.

Funding

This research received no specific grant from any funding agency in the public, commercial, or not-for profit sectors.

Institutional Review Board Statement

Not applicable.

Informed Consent Statement

Not applicable.

Data Availability Statement

All the data were created during the current study. It will be available from the corresponding author on reasonable request.

Acknowledgments

The authors acknowledge Principal, Mithibai College, Mumbai, for carrying out experimental work, Icon lab Sanpada Navi Mumbai for SEM analyses and University of Mumbai for FTIR and XRD analyses.

Conflicts of Interest

The authors declare that they have no competing interests.

References

[1] Balamurugan, S., Balu, A.R., Usharani, K., et al., 2016. Synthesis of CdO nanopowders by a simple soft chemical method and evaluation of their antimicrobial activities. Pacific Science Review A: Natural Science and Engineering. 18(3), 228–232. DOI: https://doi.org/10.1016/j.psra.2016.10.003

[2] Shiri, Z.G., Zebarjad, S.M., Janghorban, K., 2010. A study on the role of electrospinning parameters on the morphology of nickel oxide nano-belts. Materials Research Express. 6(11), 1150–1158. DOI: https://doi.org/10.1088/2053-1591/ab33bc

[3] Li, S., Lin, M.M., Toprak, M.S., et al., 2019, Nanocomposite of polymer and inorganic nanoparticles for optical and magnetic applications. Nano Reviews. 1(1), 1–22. DOI: https://doi.org/10.3402/nano.v1i0.5214

[4] Farbod, M., Kajabafvala, M., 2013. Effect of nanoparticle surface modification on the adsorption-enhanced photocatalysis of Cd/TiO_2 nanocomposite. Powder Technology. 239(1), 434–440. DOI: https://doi.org/10.1016/j.powtec.2013.02.027

[5] Al-Douri, Y., Khan, M.M. & Jennings, J.R. , 2023, Synthesis and optical properties of II–VI semiconductor quantum dots: a review. *J Mater Sci: Mater Electron* **34**, 993. https://doi.org/10.1007/s10854-023-10435-5

[6] Biette, L., Carn, F., Maugey, M., et al., 2005. Macroscopic Fibers of Oriented Vanadium Oxide Ribbons and Their Application as Highly Sensitive Alcohol Microsensors. Advanced Materials. 17, 2970–2974. DOI: https://doi.org/10.1002/adma.200501368

[7] Zhou, C., Mai, L., Liu, Y., et al., 2007. Synthesis and Field Emission Property of $V_2O_5 \cdot nH_2O$ Nanotube Arrays.The Journal of Physical Chemistry C. 111(23), 8202–8205. DOI: https://doi.org/10.1021/jp0722509

[8] Le, T.K., Kang, M., Kim, S.W., 2019. A review on the optical characterization of V_2O_5 micro-nanostructures. Ceramics International. 45(13), 15781–15798. DOI: https://doi.org/10.1016/j.ceramint.2019.05.339

[9] Borhade, A.V., Uphade, B.K., 2016. Removal of chromium (VI) from aqueous solution using modified CdO nanoparticles. Desalination and Water Treatment. 57(21), 9776–9788. DOI: https://doi.org/10.10

80/19443994.2015.1041051

[10] Shanmugam, N., Saravanan, B., Reagan, R., et al., 2014. Effect of Thermal Annealing on the $Cd(OH)_2$ and Preparation of Cdo Nanocrystals. Modern Chemistry & Applications. 2(1), 1000124. DOI: https://doi.org/10.4172/2329-6798.1000124

[11] Muhammad Munir Sajid, Naveed Akthar Shad, Yasir Javed, Sadaf Bashir Khan, Zhengjun Zhang, Nasir Amin, Haifa Zhai,, 2020, Preparation and characterization of Vanadium pentoxide (V2O5) for photocatalytic degradation of monoazo and diazo dyes, Surfaces and Interfaces, 19,100502,ISSN 2468-0230, https://doi.org/10.1016/j.surfin.2020.100502.

[12] Ferro, R., Rodríguez, J.A., Bertrand, P., 2002. Mixed $(ZnO)_X (CdO)_{1-X}$ policrystalline oxide films deposited by spray pyrolysis from metal nitrate solutions. Journal of Materials Science Letters. 21, 1939–1941. DOI: https://doi.org/10.1023/A:1021660730842

[13] Ristic, M., Poporic, S., Music, S., 2004. Formation and properties of $Cd(OH)_2$ and CdO particles. Materials Letters. 58(20), 2494–2499. DOI: https://doi.org/10.1016/j.matlet.2004.03.016

[14] Reddy, C.V., Babu, B., Shim, J., 2018. Synthesis, optical properties and efficient photocatalytic activity of CdO/ZnO hybrid nanocomposite. Journal of Physics and Chemistry of Solids. 112, 20–28. DOI: https://doi.org/10.1016/j.jpcs.2017.09.003

[15] Qi, J., Feng, Y., Yu, J., et al., 2025. Wave-like Cu substrate with gradient {100} texture for anode-free lithium batteries. Energy Storage Materials. 77, 104176. DOI: https://doi.org/10.1016/j.ensm.2025.104176

[16] Gopidas, K.R., Bohorquez, M., Kamat, P.V., 1990. Photophysical and photochemical aspects of coupled semiconductors: charge-transfer processes in colloidal cadmium sulfide-titania and cadmium sulfide-silver(I) iodide systems. The Journal of Physical Chemistry. 94(16), 6435–6440. DOI: https://doi.org/10.1021/j100379a051

[17] Das, S., 2016. Hierarchical nanostructured ZnO-CuO nanocomposite and its photocatalytic activity. Journal of Nano Research. 35, 21–26. DOI: https://doi.org/10.4028/www.scientific.net/jnanor.35.21

[18] Kannan, Y.B., Saravanan, R., Srinivasan, N., et al., 2016. Synthesis and characterization of some ferrite nanoparticles prepared by co-precipitation method. Journal of Materials Science: Materials in Electronics. 27, 12000–12008. DOI: https://doi.org/10.1007/s10854-016-5347-y

[19] Nayak, J., Sahu, S.N., Kasuya, J., et al., 2008. Effect of Substrate on the Structure and Optical Properties of ZnO Nanorods. Journal of Physics D: Applied Physics. 41(11), 115303–115308. DOI: https://doi.org/10.1088/0022-3727/41/11/115303

[20] Ibrahim Khan, Khalid Saeed, Idrees Khan, 2019, Nanoparticles: Properties, applications and toxicities, Arabian Journal of Chemistry, 12(7), 908-931, https://doi.org/10.1016/j.arabjc.2017.05.011.

[21] Sebastian, S., Diana, P., Ganesh, V. *et al.* Synthesis and characterization of Fe-doped CdO nanoparticles via a coprecipitation method: application as a promising photodetector. *Appl. Phys. A* **131**, 160 (2025). https://doi.org/10.1007/s00339-025-08270-y

[22] Prashanna Suvaitha, S, 2025. Novel trimetallic oxide ($CdO/ZnO/V_2O_5$) nanocomposite derived from eggshell membrane: Synthesis, structural characterization, antibacterial and antifungal activities. Surfaces and Interfaces. 56, 105677. DOI: https://doi.org/10.1016/j.surfin.2024.105677

[23] Tadjarodi, A., Imani, M., Kerdari, H., 2013. Experimental design to optimize the synthesis of CdO cauliflower-like nanostructure and high performance in photodegradation of toxic azo dyes. Materials Research Bulletin. 48(3), 935–942. DOI: https://doi.org/10.1016/j.materresbull.2012.11.042

[24] Dhatshanamurthi, P., Subash, B., Shanthi, M., 2015. Investigation on UV-A light photocatalytic degradation of an azo dye in the presence of CdO/TiO_2 coupled semiconductor. Materials Science in Semiconductor Processing. 35, 22–29. DOI: https://doi.org/10.1016/j.mssp.2015.02.069

[25] Millesi, S., Schilirò, M., Greco, F., et al., 2016. Nanostructured CdO thin films for water treatments. Materials Science in Semiconductor Processing. 42(Part 1), 85–88. DOI: https://doi.org/10.1016/j.mssp.2015.08.005

[26] Khan, S.S., 2015. Enhancement of visible light photocatalytic activity of CdO modified ZnO nanohybrid particles. Journal of Photochemistry and Photobiology B: Biology. 142, 1–7. DOI: https://doi.org/10.1016/j.jphotobiol.2014.11.001

[27] Al-Ghamdi, A.A., Abdel-wahab, M.S., Farghali, A.A., et al., 2016. Structural, optical and photo-catalytic activity of nanocrystalline NiO thin films. Materials Research Bulletin. 75, 71–77. DOI: https://doi.org/10.1016/j.materresbull.2015.11.027

[28] Kaneva, N.V., Dimitrov, D.T., Dushkin, C.D., 2011. Effect of nickel doping on the photocatalytic activity of ZnO thin films under UV and visible light. Applied Surface Science. 257(18), 8113–8120. DOI: https://doi.org/10.1016/j.apsusc.2011.04.119

[29] Arockia Anushya, S., Philominal, A., 2024. Efficient photocatalytic degradation of crystal violet using quaternized reduced graphene oxide nanocomposite. Diamond and Related Materials. 149, 111592. DOI: https://doi.org/10.1016/j.diamond.2024.111592

[30] Raees, A., Jamal, M., Ahmad, I., et al., 2021. Synthesis and Characterization of CeO_2/CuO Nanocomposites for Photocatalytic Degradation of Methylene Blue in Visible Light. Coatings. 11(3), 305. DOI: https://doi.org/10.3390/coatings11030305

[31] Mansoori, S.M., Yamgar, R.S., Rathod, S.V., 2021. Photocatalytic Degradation of Methylene Blue Dye Using Synthesized CuO:CdO Nanocomposite. Journal of Scientific Research. 65(6), 66–71. DOI: https://doi.org/10.37398/JSR.2021.650609

[32] Balamurugan, S., Balu, A.R., Usharani, K., et al., 2016. Synthesis of CdO nanopowders by a simple soft chemical method and evaluation of their antimicrobial activities. Pacific Science Review A: Natural Science and Engineering. 18(3), 228–232. DOI: https://doi.org/10.1016/j.psra.2016.10.003

[33] Ganesan, S., Gurunathan, R., Pasupuleti, R.R., et al., 2023. Green synthesis of V_2O_5/ZnO nanocomposite materials for efficient photocatalytic and anti-bacterial applications. Applied Nanoscience. 13, 859–869. DOI: https://doi.org/10.1007/s13204-021-01923-3

[34] Chan, S.H.S., Yeong Wu, T., Juan, J.C., et al., 2011. Recent developments of metal oxide semiconductors as photocatalysts in advanced oxidation processes (AOPs) for treatment of dye wastewater. Journal of Chemical Technology & Biotechnology. 86, 1130–1158. DOI: https://doi.org/10.1002/jctb.2636

[35] Gupta, R., Eswar, N.K., Modak, J.M., et al., 2018. Ag and CuO impregnated on Fe doped ZnO for bacterial inactivation under visible light. Catalysis Today. 300, 71–80. DOI: https://doi.org/10.1016/j.cattod.2017.05.032

[36] Liu, J., Jin, J., Deng, Z., et. al., 2021. Nanostructures for enhanced photocatalytic property. Journal of Colloid and Interface Science. 384(1), 1–9. DOI: https://doi.org/10.1016/j.jcis.2012.06.044

[37] Pirhashemi, M., Habibi-Yangjeh, A., Rahim Pouran, S., 2018. Review on the criteria anticipated for the fabrication of highly efficient ZnO-based visible-light-driven photocatalysts. Journal of Industrial and Engineering Chemistry. 62, 1–25. DOI: https://doi.org/10.1016/j.jiec.2018.01.012

[38] Herrmann, J.M., 1999. Heterogeneous photocatalysis: fundamentals and applications to the removal of various types of aqueous pollutants. Catalysis Today. 53, 115–129. DOI: https://doi.org/10.1016/S0920-5861(99)00107-8